ACS Sustainable Chemistry & Engineering

pubs.acs.org/journal/ascecg

Research Article

Aqueous-Based Recycling of Cellulose Nanocrystal/Chitin Nanowhisker Barrier Coatings

Yue Ji, D. Eric Shen, Yang Lu, Gregory T. Schueneman, Meisha L. Shofner, and J. Carson Meredith*

Cite This: *ACS Sustainable Chem. Eng.* 2023, 11, 10874−10883

Read Online

ACCESS | Metrics & More | Article Recommendations | Supporting Information

ABSTRACT: Multilayer films consisting of nanocellulose and nanochitin as oxygen barrier coatings and a conventional petroleum-based moisture barrier plastic as the substrate have been widely studied for food packaging applications. A challenge with enabling recycling of such hybrid multilayer materials is separating the coating from the substrate. In this work, we studied multilayer films consisting of poly(ethylene terephthalate) (PET) as a model substrate with chitin nanowhiskers (ChNWs) and cellulose nanocrystals (CNCs) as bilayer barrier coatings. Dissolution in aqueous media at different pH values was utilized for coating removal. PET coated with bilayers of recycled CNC and ChNW had an oxygen permeability (OP) of 6.6 $cm^3 \cdot \mu m/m^2/day/kPa$. It had a 27% increase compared to PET with the original bilayer coatings (5.2 $cm^3 \cdot \mu m/m^2/day/kPa$) while still provided a 62% reduction compared to uncoated PET (17.3 $cm^3 \cdot \mu m/m^2/day/kPa$). Additionally, single-layer coatings of CNC were recycled for up to three runs, and no significant difference was found in the OP values for the films with recycled CNC coatings. This study demonstrates a pathway for recycling of the relatively expensive coating, which may provide a more sustainable solution for production of food packages.

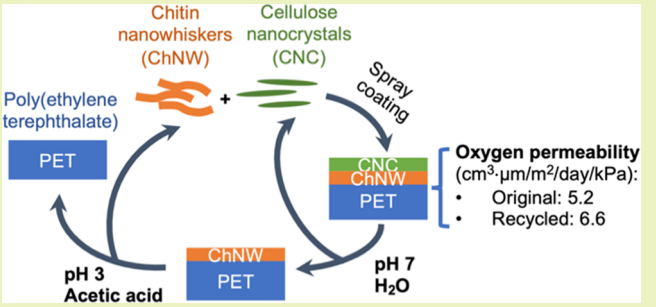

KEYWORDS: *recycling, cellulose nanocrystals, chitin nanowhiskers, gas barrier, multilayer coatings, selective solvent dissolution*

INTRODUCTION

Packaging materials are ubiquitous in modern life because they maintain the safety, quality, and integrity of food, pharmaceutical, and cosmetic products.[1] High gas barrier properties, particularly for oxygen and moisture, are desired for packaging applications that decelerate the deterioration of food and other products. Currently, the most widely used materials in barrier packaging are multilayer packages containing multiple different polymers, such as of polyolefins, poly(vinyl chloride) (PVC), poly(ethylene terephthalate) (PET), and ethylene vinyl alcohol copolymer (EVOH).[2] However, these are mainly derived from nonrenewable resources (petroleum) and are not biodegradable.[3] Though PET and polyolefins can be synthesized from renewable sources,[4] this has not become widespread commercially and they are nonbiodegradable. In addition, because high-performance barrier packages are usually used in a multilayer structure and each individual layer has a different function (e.g., barrier property, antibacterial property, printability, adhesive, etc.), recycling of such packaging materials requires the separation between layers, which constrains the recycling of multilayer plastics. Thus, the use of these plastics has resulted in many end-of-life problems, such as pollution and hazards to human, wildlife, and environmental health, which includes greenhouse gas emissions associated with producing new virgin plastics to replace those that are not recovered, recycled, or upcycled.[5]

To address these problems, researchers have become interested in applying bio-based materials for packaging applications. Cellulose and chitin, which are the most abundant polysaccharides in nature, are two of the most promising alternatives. Cellulose consists of D-glucose units and is rich in wood cell walls, while chitin consists of *N*-acetyl-D-glucosamine units and is mainly sourced from exoskeletons of shellfish and fungi.[6,7] Cellulose and chitin have high crystallinity due to their strong intermolecular hydrogen bonding, and their nanomaterials have low oxygen permeabilities (OPs) when processed into films or coatings. Examples of these nanomaterials are cellulose nanofibrils (CNFs),[8] cellulose nanocrystals (CNCs),[9,10] chitin nanowhiskers (ChNWs),[11,12] and chitin nanofibers (ChNFs).[9,13] They have been widely studied to be applied as fillers in matrices, free-standing films, and coatings on substrates to function as oxygen barriers.[14]

Because nanochitin is usually cationic due to deacetylation treatment and nanocellulose is usually anionic due to acid

Received: April 25, 2023
Revised: June 27, 2023
Published: July 13, 2023

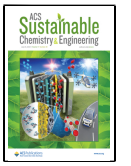

hydrolysis or (2,2,6,6-tetramethylpiperidin-1-yl)oxyl (TEMPO) oxidation, the electrostatic attraction between them promotes densification at their interface and improves the oxygen barrier properties.[15−22] For instance, a cellulose acetate (CA) film coated with a bilayer of ChNW and CNC had an OP that was 99, 22, and 84% lower than those of uncoated CA and CA coated with a single layer of ChNW or CNC, respectively.[19] However, there remains much room for improvement in the water vapor barrier property to satisfy the requirements for food packaging applications.[19−21] Furthermore, cellulose and chitin are sensitive to humidity, and their gas barrier properties decrease significantly with elevated relative humidity (RH).[20,23] One approach to address these issues with water vapor in cellulose and chitin oxygen barriers is to use a conventional moisture barrier material as the substrate.[15,17] A drawback of this approach is the fact that most of the high-performing conventional water vapor barriers are petroleum-based and nondegradable. Promoting deconstruction of the coating and substrate at the end of life could enable recycling of the packaging materials to manage the dilemma.

One method that has been proposed for deconstructing multilayer plastic film is selectively dissolving targeted layers.[24,25] A series of solvents is used to separate and recycle each plastic layer by solvent wash, filtration, and antisolvent in sequence. In many cases, aqueous basic wash steps are already part of treating recycled plastic, whether rigid or film.[26,27] Selective solvent dissolution methods could be applied to recover the chitin and cellulose oxygen barrier layers if they were coated onto a more hydrophobic water barrier substrate. For instance, previous work in our group showed that a 1 M sodium hydroxide solution can be used to remove ∼80% of a bilayer coating consisting of a layer of CNCs, followed by a blend of ChNW and chitosan (i.e., highly deacetylated chitin) from PET.[22] Since the current costs of PET, CNC, and chitin are ∼0.45,[28] 10−50,[29] and ∼8 dollars per pound,[30] respectively, recycling of the more costly CNC and ChNW coating layers may support the economics of CNC and ChNW utilization as well. However, it remains unknown how to achieve separation between the two CNC and ChNW coating layers and how the properties of the coating materials will be influenced during their recovery and recoating.

In our work, we applied the solvent dissolution method for the first time to separate and recycle ChNW and CNC that were spray coated on PET substrates. PET was selected as the model substrate because both mechanical and chemical routes to its recycling exist, and it is commonly used in food packaging, even though today recycling of PET film is very limited. The intention here is to use PET as a model for assessing the ability to remove cellulose- and chitin-based barrier coatings and assess their barrier performance after recoating their recyclate. The coatings can be separated by treatment with water and acetic acid solution to remove the CNC and the ChNW layers in sequence, respectively. The recovered materials were redispersed to form homogeneous suspensions, which were spray coated on PET again as oxygen barriers. The original and recycled suspensions were examined in terms of ζ potential, hydrodynamic radius, crystallinity, optical properties, and rheological properties. The PET films coated with original or recycled materials were characterized in terms of oxygen and water vapor barrier and optical properties. Though recycling caused a slight loss of the oxygen barrier property of CNC, the PET coated with recycled materials as a bilayer had an OP 62% lower than that of uncoated PET, which meets the requirement for packaging many types of food. This study proposes recycling the relatively expensive renewable barrier coatings and enables future recycling of the PET substrates, which is beneficial to improve sustainability in the production of packaging materials.

EXPERIMENTAL METHODS

Materials. PET substrates (SM30C) with a density of 1.4 g/cm^3 were supplied by SKC Inc. To prepare the ChNWs, chitin flakes (Tidal Vision) were deacetylated with 40 wt % sodium hydroxide (NaOH; ACS grade, Sigma-Aldrich) solution at an oil-bath temperature of 155 °C for 140 min and homogenized to form a 0.5 wt % ChNW suspension by the same method as previously reported.[19] A 10 wt % CNC slurry with Na^+ as counterions was supplied by USDA Forest Products Laboratory (FPL) and was diluted to 0.5 wt % with deionized water for coating. The CNCs were derived from commercial softwood prehydrolysis Kraft dissolving pulp. The properties for ChNW and CNC are available in Tables S1 and S2, respectively. Acetic acid (HOAc; ACS grade) and magnesium nitrate ($Mg(NO_3)_2$) were purchased from Sigma-Aldrich and used without further purification.

Spray Coating. Four different samples were prepared, including PET films coated with a bilayer of ChNW as the bottom layer and CNC as the top layer, and three control samples: PET films coated with a single layer of ChNW, CNC, or a blend of ChNW and CNC with a 1:1 mass ratio. These coated films are referred to as PET-ChNW-CNC, PET-ChNW, PET-CNC, and PET-blend, respectively.

The suspensions were spray coated on the PET substrate by using the same setup as we previously reported.[21] Briefly, the PET film was fixed along its four edges to a hot plate that was held vertically and maintained at 80 °C during the spray-coating process. For the PET-ChNW-CNC film, a volume of 25 mL of 0.5 wt % ChNW or 25 mL of 0.5 wt % CNC was spray coated on a 19 cm × 19 cm PET film in sequence. For PET-ChNW and PET-CNC films, 25 mL of either suspension was applied; for the PET-blend film, 25 mL of ChNW and 25 mL of CNC were mixed by stirring for 30 min and sonicated at 40% amplitude for 1 min using a QSonica sonicator ultrasonic processor (Q500), and a total of 50 mL of blend was coated onto the substrate. Between subsequent sprays, the sprayed liquid was dried for 1 min. After the coating was dried, the coated film was exposed to room atmosphere (∼50% RH) for one day and then conditioned at ∼53% RH in a sealed container with saturated $Mg(NO_3)_2$ solution used to maintain the RH at room temperature for 7 days.

Recycling of the Coating Materials. Two solvents were selected for recycling the coating materials: deionized water for CNC layers and an aqueous solution of HOAc at pH = 3 for ChNW layers or blends. The PET-ChNW-CNC films were cut into small pieces (2−3 cm × 2−3 cm), soaked in 60 mL of water, stirred for ∼6 h, and removed from the solution to separate the CNC layer. The resulting films were then treated with pH 3 HOAc solution following the same steps as the water treatment for recycling CNC to recycle the ChNW layer. The washed films were rinsed twice using a total of 40 mL of water, and the washing water was added to the 60 mL of water or HOAc solution in the first washing step. The dispersions were concentrated at 60 °C to ∼25 mL and dried in a room atmosphere to obtain dry, recycled CNC and ChNW in sequence. The recycled material was weighed, redispersed in the same solvent (e.g., water for CNC, pH 3 HOAc for ChNW) with a 0.5 wt % solid content, and stirred for ∼6 h. The suspension was then sonicated at 40% amplitude for 1 min to obtain a homogeneous suspension. The recycled materials are referred to as rCNC2 and rChNW2, where the letter "r" means "recycled" and the number "2" indicates that the materials were recycled from a "bilayer coating".

For the single-layer-coated films, a one-step treatment with one solvent was applied for separating the coating layer, such as water for PET-CNC and pH 3 HOAc solution for PET-ChNW and PET-blend. The suspensions of the recycled materials were prepared with the same method as described above. These recycled materials are

https://doi.org/10.1021/acssuschemeng.3c02457
ACS Sustainable Chem. Eng. 2023, 11, 10874−10883

referred to as rCNC1, rChNW1, and rblend, where the number "1" indicates that the materials were recycled from a "single layer".

The recycled materials were spray coated on PET substrates with the same method as described above to obtain PET-rCNC1, PET-rChNW1, PET-rChNW2-rCNC2, and PET-rblend films for comparison of film properties.

To study the influence of multiple recycle runs on the film properties, CNC-coated PET films were selected as a model film, and the coating on PET-rCNC1 was recycled and recoated for multiple rounds using the same methods as described above. The materials recycled for two or three rounds are referred to as 2rCNC1 and 3rCNC1, respectively, and the coated films are referred to as PET-2rCNC1 and PET-3rCNC1, respectively.

Characterization. The original and recycled suspensions were characterized using similar methods as previously reported.[19] The suspensions were diluted to 0.025 wt % using the same solvent and subjected to dynamic light scattering (DLS; DynaPro NanoStar, Wyatt Technology Corporate) at 25 °C to obtain the hydrodynamic radii. The ζ potential values of suspensions were measured using a Zetasizer Nano ZS (Malvern Panalytical), where ChNW suspensions and blends were diluted to 0.025% by pH 3 HOAc, and CNC suspensions were diluted to 0.025 wt % with a 5 mM NaCl solution. The viscosities of the 0.5 wt % suspensions were characterized using an MCR302 rheometer (Anton Paar) at 23 °C by using a cone-plate geometry. The cone is 49.957 mm in diameter (cone angle 0.977°, truncation 0.094 mm), and the bottom plate insert has a diameter of 50 mm. The compositions of the suspensions were characterized by elemental analysis of nitrogen and sulfur contents using a Carlo Erba 1108 analyzer at Atlantic Microlab. The light transmittance spectra for suspensions were measured using a Shimadzu UV-1800 spectrometer. Fourier transform infrared (FT-IR) spectra for air-dried suspensions were obtained using a Nicolet 6700 spectrometer equipped with a diamond crystal attenuated total reflectance (ATR) attachment. The crystalline structure of the nanocrystals or nanowhiskers was characterized by X-ray diffraction (XRD) using an X'Pert PRO α-1 X-ray diffractometer (Malvern Panalytical), and crystallinity values for ChNW, rChNW1, CNC, and rCNC1 were calculated using empirical equations.[31,32] Details of XRD are available in the Supporting Information.

The film properties were characterized using the same methods as previously reported.[21] The thicknesses were measured with a digital micrometer (Coolant Proof Micrometer Series 293, Mitutoyo). The cross-sectional structures for the coatings were obtained by imaging with scanning electron microscopy (SEM; SU8010, Hitachi High-Tech Corp.). The OP values of the coated films were measured by using a Class 230 Oxygen Transmission Rate Test System (Labthink International, Inc.) at 23 °C and 50% relative humidity (RH) for the O_2 side and 0% RH for the N_2 side. The water vapor transmission rate (WVTR) was measured by a PERMATRAN-W 1/50 instrument (MOCON) at 23 °C and 50% RH for the permeant side and 5% RH for the dry side. The light transmittance and haze were measured using an integrating sphere (DRA 2500) by following ASTM D1003. To verify the removal of the coatings with different solvents, the coated films before and after washing were characterized using a Shimadzu IRAffinity-1 FT-IR spectrometer with an ATR attachment.

RESULTS AND DISCUSSION

Selection of Solvents. The CNC and ChNW that were spray coated onto PET substrates as a bilayer were recycled by selective aqueous solvent dissolution, as is shown in Figure 1. Water was used for recycling the CNC layer and an aqueous solution of HOAc (pH = 3) was used for recycling the ChNW layer. As a qualitative measure of the efficiency of the solvents for coating recycling, the FT-IR spectra for the coated films before and after being treated with H_2O or HOAc solution are shown in Figure 2. Coated PET films without solvent treatment showed a broad peak at ~3300 cm^{-1} which is assigned to O−H stretching for CNC and ChNW and N−H

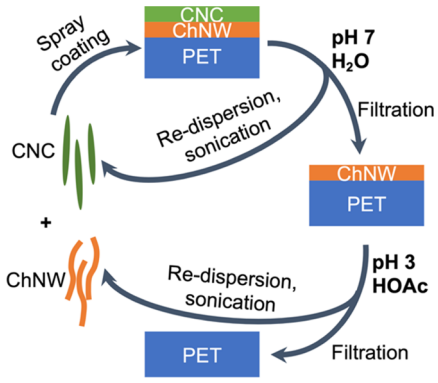

Figure 1. Schematic of idealized recycling of ChNW and CNC coatings from a bilayer-coated PET film.

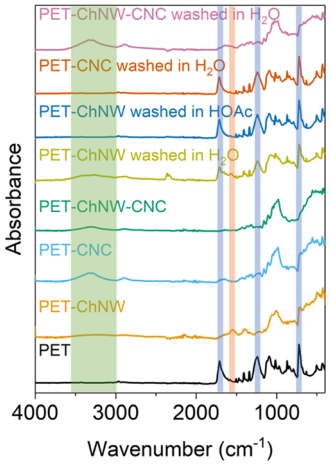

Figure 2. FT-IR spectra for coated PET films and those washed in H_2O or HOAc solution as a comparison to uncoated PET. Peaks in green (~3300 cm^{-1}) are assigned to O−H stretching for CNC and ChNW and N−H stretching for ChNW only. Peaks in blue are characteristic peaks for PET: 1711 cm^{-1} (C═O stretching in phenyl ester groups), 721 cm^{-1} (C═C bending), and 1240 cm^{-1} (C−O stretching in aromatic ester). Peaks in orange are the characteristic peaks for ChNW at 1623 cm^{-1} (N−H bending).

stretching for ChNW only. The characteristic peaks for ChNW and CNC were observed at 1623 cm^{-1} (N−H bending) and 1205 cm^{-1} (S═O stretching of sulfate half-ester groups), respectively. For PET, three characteristic peaks were observed at 1711 cm^{-1} (C═O stretching in phenyl ester groups), 721 cm^{-1} (C═C bending), and 1240 cm^{-1} (C−O stretching in aromatic ester). By comparing washed PET-ChNW with PET and original PET-ChNW, it is found that both H_2O and HOAc removed some ChNW, and the PET substrates became exposed; however, there remained some ChNW on the surface when H_2O was applied as the solvent, as evidenced by the characteristic peaks for ChNW at ~3300 and 1623 cm^{-1}, which were not observable in the spectrum for PET-ChNW washed in HOAc solution. HOAc solution is a more effective solvent for removing ChNW because ChNWs are protonated in acidic media, which causes interparticle electrostatic repulsion and stabilizes ChNWs in the suspension by preventing aggregation. Meanwhile, H_2O is an effective solvent for removing the CNC layer due to its high dispersibility at neutral pH,[33] as indicated by the disappearance of characteristic peaks for CNCs in the washed PET-CNC sample, e.g., peaks at ~3300 cm^{-1} and 1205 cm^{-1}. Because H_2O

https://doi.org/10.1021/acssuschemeng.3c02457
ACS Sustainable Chem. Eng. 2023, 11, 10874−10883

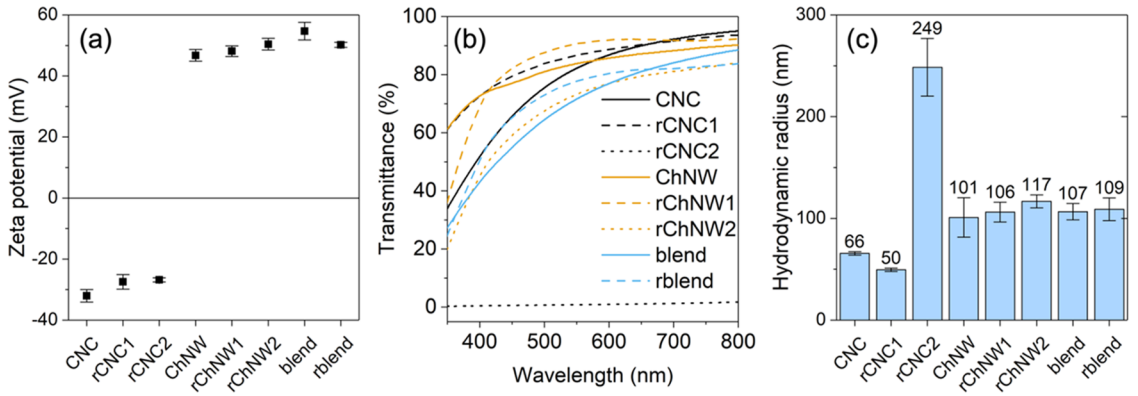

Figure 3. ζ Potential values (a), transmission spectra (b), and hydrodynamic radii (c) for original and recycled CNC, ChNW suspensions, and blends.

redispersed CNC more efficiently than ChNW, it was selected for recycling the CNC layer; HOAc solution was selected for recycling the layers containing ChNW, including single-layer coatings of ChNW, the ChNW layer in ChNW-CNC bilayers, and the blended coatings of ChNW and CNC. The calculated efficiencies (i.e., the mass ratio of dry, recycled material to dry, coated material) for recycling materials from single-layer coatings (i.e., rCNC1, rChNW1, and rblend) were 90−100% due to the high dispersity of the materials in relative selected solvents. The efficiencies for recycling rCNC2 and rChNW2 from bilayer coatings were 30−60% and 140−150%, respectively. The lower recycling efficiency for CNC and the higher value for ChNW compared to those in single layers were likely due to the penetration of CNC in the ChNW layer at their interface. This penetration has been observed by energy-dispersive X-ray spectroscopy (EDS) in our previous study.[19] The washing conditions (e.g., type of solvent, washing time) were probably not intense enough to redisperse all CNC from bilayers, resulting in overestimation of recycling efficiency for ChNW. The existence of CNC in rChNW2 was verified by elemental analysis, FT-IR, and XRD discussed in the following section.

Properties of Suspensions. Elemental analysis results suggested (Table S3) the mixing of CNC and ChNW in rChNW2 and rCNC2. Nitrogen and sulfur are characteristic elements in ChNW and CNC, respectively. By comparing the N and S contents in rChNW2 and rCNC2 with those in ChNW and CNC, it is calculated that rChNW2 contained 69 ± 2% ChNW and 30 ± 5% CNC, while rCNC2 contained 4 ± 1% ChNW and 92 ± 9% CNC. The mixing of CNC and ChNW in rChNW2 and rCNC2 was also qualitatively verified by FT-IR (Figure S1), where the characteristic peak for ChNW (1543 cm^{-1} for N−H bending) occurred in rCNC2 and the peak for CNC (1236 cm^{-1} for S═O stretching) occurred in rChNW2. Furthermore, the minor changes in the N content of rChNW1 (compared to ChNW) and the S content of rCNC1 (compared to CNC) indicated their stability to heat- or sonication-induced degradation during the recycling process.

The recycled suspensions were generally stable in the solvents after redispersion and sonication, similar to the original materials. The ζ potential value is a measure of the stability of colloidal dispersions, and a general guideline is that nanoparticles with absolute ζ potential values greater than 30 mV or ranging from 20 to 30 mV are considered highly stable or moderately stable in suspensions.[34] As shown in Figure 3a, the original and recycled ChNW suspensions and blends all had ζ potential values greater than +45 mV at pH = 3 and an ionic strength of 2 mM; CNC, rCNC1, and rCNC2 suspensions had ζ potential values of −32.1 ± 2.1, −27.5 ± 2.4, and −26.8 ± 0.7 mV, respectively, in 5 mM NaCl solution (at pH = 7, ionic strength of 6 mM). Thus, suspensions in this study are all considered stable. The absolute ζ potential values for CNC and the blend slightly decreased after recycling, which was not observed for ChNW. Given that CNC is stable to the removal of sulfate half-ester groups under neutral conditions even when heated at 85 °C for 3 days,[35] which is also verified by elemental analysis results, this decrease in ζ potential is not attributed to a change in charge density of CNC (i.e., arising from a change in the sulfate half-ester group concentration). It is likely because the never-dried original CNC has a gel layer containing more ions of low-molecular-weight organic compounds originating from the hydrolysis process, but drying and sonication during the coating and recycling processes resulted in the release of these ions.[36,37] This expands the electrical double layer and causes the decrease in absolute ζ potential values for CNC and the blend. ChNW, in contrast, was dried after deacetylation and before being homogenized into a suspension, which likely explains the lack of decrease in ChNW ζ potential after washing and recoating.

Most original and recycled suspensions had high transmittances, except rCNC2, as shown in Figures 3b and S2. The transmittance became lower at shorter wavelengths due to the absorbance in the UV tailing into the visible spectrum by sulfate half-ester groups in CNC (~270 nm) and amide groups in ChNW (~230 nm).[38−40] For recycled single-layer coatings, e.g., rCNC1, rChNW1, and rblend, their average transmittance in the range of 350−800 nm slightly increased from 78 to 85, 82 to 85, and 69 to 72% in comparison to the original materials, respectively. The rCNC1 and rblend showed higher transmittance at shorter wavelengths compared to the original materials but lower transmittance at longer wavelengths; however, the rChNW1 compared to the original ChNW showed the opposite phenomenon. Such a phenomenon has also been found for CNC suspensions that were homogenized with an Ultra-Turrax disperser, with or without a following step of ultrasonication in a bath.[40] It is likely the result of drying and sonication, which may cause changes in the chemical environment (e.g., the release of ions into the solvent for CNC), H bonding, and crystalline structure (for ChNW, will be explained along with Figure 4 later). However, for rCNC2 and rChNW2, the average transmittance values

https://doi.org/10.1021/acssuschemeng.3c02457
ACS Sustainable Chem. Eng. 2023, 11, 10874−10883

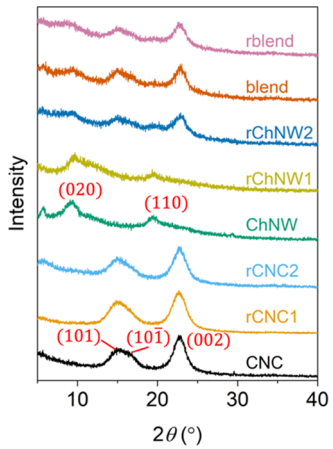

Figure 4. XRD patterns of drop-cast films of original and recycled CNC and ChNW layered samples and blends.

decreased to 1 and 69%, respectively, with the rCNC2 suspension becoming extremely hazy and white in color (Figure S2). This may be caused by the dissolution of ChNW in rCNC2 and CNC in rChNW2 during recycling, resulting in aggregation between oppositely charged ChNWs and CNCs and increased particle size in the suspension, which caused stronger Mie scattering where the intensity of scattered light is inversely proportional to the square of the particle radius.[41] Here, Mie scattering rather than Rayleigh scattering is believed to be the main cause because the hydrodynamic radii for nanoparticles in this work are in the range of 50−250 nm, suggesting a size factor ($x = 2\pi r/\lambda$, where r is the particle radius and λ is the wavelength of the light) close to or greater than 1.[41] Rayleigh scattering is valid for particles with dimensions far shorter than the wavelength of light ($x \ll 1$). The decrease in transmittance may have been especially pronounced for rCNC2 because ChNW became less charged under neutral conditions, which caused more obvious particle aggregation.

The change in nanoparticle size was verified by DLS. As is shown in Figure 3c, the hydrodynamic radius (R_h) for rCNC2 was significantly higher than the R_h values of the other samples due to aggregation caused by the dissolution of ChNW. The change in R_h was more significant for rCNC2 compared to the original CNC than for rChNW2 compared to the original ChNW, although there was more CNC in rChNW2 than ChNW in rCNC2 (shown by elemental analysis). This is likely because CNCs still disperse uniformly in pH 3 HOAc solution (in rChNW2) since the pK_a of sulfate groups is 1.9.[42] However, ChNW cannot disperse stably at pH 7 due to deprotonation of $-NH_3^+$[43] and significant aggregation occurred in rCNC2. In addition, rCNC1 had a smaller R_h than CNC, which is also probably due to the release of ions in the gel layer of CNC during sonication that expanded the electrical double layer.[36] The R_h did not significantly decrease for rChNW1 and rblend compared to the original ChNW and blend probably because, similar to the ζ potential change, the electrical double layer of ChNW was not significantly affected by recycling. Additionally, though CNC and ChNW had similar average lengths as measured by atomic force microscopy (Tables S1 and S2), the R_h of CNC was significantly smaller than the R_h of ChNW. This discrepancy is because different solvents were used for DLS measurements, i.e., H_2O for CNC and HOAc solution for ChNW, where different ionic strengths and pH altered the diffusion behavior of the nanoparticles.[44]

The structure of CNCs and ChNWs was affected differently by recycling. CNCs maintained high crystallinity after recycling, while ChNWs became less ordered. As shown in Figure 4, for ChNW, the diffraction peaks at $2\theta = 9°$ and 19.4° correspond to the (020) and (110) crystallographic planes,[45] respectively; for CNC, the diffraction peaks at 2θ = 15, 16.4, and 22.7° correspond to the (101), (10$\bar{1}$), and (002) crystallographic planes,[46] respectively. In previous reports using powdered samples, there were additional peaks beyond those observed in this work, such as peaks indexed as (021), (120), (130), and (013) at 2θ = 13, 21, 23, and 26.4° for chitin,[45] and peaks indexed as (021) and (040) at 2θ = 21 and 34.5° for cellulose.[46] These peaks were not observed in this work probably because chitin and cellulose were chemically treated, i.e., deacetylated or hydrolyzed, respectively, and were separated into discrete nanoparticles before characterization. Changes in structural order were assessed using the crystallinity indices (CrIs). The CrIs for ChNW and rChNW1 were 29 and 12%, respectively. These values were significantly lower than those for typical ChNFs (with higher aspect ratios deacetylated under less aggressive conditions) or chitin nanocrystals (ChNCs, usually prepared by acid hydrolysis or TEMPO oxidation), e.g., ∼80 to 90%.[19,45,47] This is mainly because more aggressive deacetylation conditions caused a decrease in crystallinity and a less ordered structure.[19] The rChNW1 had a lower CrI than ChNW, which suggests a decrease in structural order after recycling. In contrast, the calculated crystallinity indices for CNC and rCNC1 were both 70%, using a similar empirical equation.[31] The crystalline structure of CNC is more resistant to redispersion than ChNW during sonication probably because of their different H-bonds: NH···O═C interchain (intrasheet) H-bonds and O(3)H···O(5) intersheet H-bonds in ChNW,[48] and only OH···O H-bonds in CNC, where OH···O H-bonds are stronger than NH···O H-bonds. Thus, the rCNC1 maintained a high CrI after recycling. Additionally, the crystalline peaks for CNC were observed in the XRD pattern for rChNW2, which also qualitatively suggests the dissolution of CNC in rChNW2. Though the dissolution of ChNW in rCNC2 was also verified by elemental analysis, rCNC2 did not show crystalline peaks for ChNW because of its low concentration.

The viscosities for all 0.5 wt % suspensions are shown in Figure S3. Sample rCNC2 showed shear-thinning behavior and a significantly higher viscosity than CNC and rCNC1. The dissolution of ChNW in rCNC2, as supported by DLS and elemental analysis results, may be an explanation.[49] The original blend also showed slight shear thinning at shear rates greater than 10 s^{-1}, though no significant increase in particle size was observed. This shear-thinning behavior was also possibly caused by a changed microstructure under shear due to interparticle attractions between ChNWs and CNCs and the hindered electrostatic repulsion among ChNWs or CNCs in the suspensions where both were present.[49] All of the other suspensions behaved as Newtonian fluids at shear rates greater than 1 s^{-1}. Additionally, except for rCNC2, the viscosities for all suspensions decreased after recycling. It has been found that sonication reduces the viscosities of never-dried CNC suspensions of different solid contents by increasing particle dispersion and reducing the dimensions of suspended particles.[50] In this work, though R_h for ChNW and blend

https://doi.org/10.1021/acssuschemeng.3c02457
ACS Sustainable Chem. Eng. 2023, 11, 10874−10883

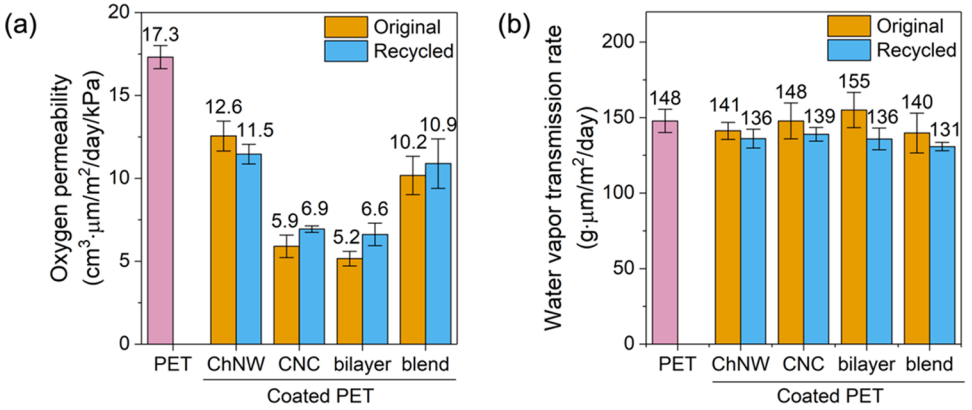

Figure 5. Oxygen permeabilities (a) and water vapor transmission rates (b) for uncoated PET and PET films coated with original or recycled ChNW and CNC materials.

samples did not significantly change after recycling, and the coating materials were dried during recycling, which likely caused the formation of interparticle bonding, the sonication promoted homogenization of the particles when they were redispersed, so their viscosities decreased after recycling.

Overall, recycling of materials from bilayer coatings (rChNW2 and rCNC2) resulted in more significant changes in suspension properties (R_h, ζ potential, viscosity) compared to materials from single-layer coatings (rChNW1, rCNC1, and rblend) due to cross-contamination. Dissolution of ChNW in rCNC2 resulted in aggregation, causing significant increases in R_h and viscosity and a decrease in suspension transparency compared to the original CNC. Though CNCs also existed in rChNW2, the differences of these suspension properties between rChNW2 and the original ChNW were less significant than the differences between rCNC2 and the original CNC due to the influence of pH (i.e., pH 3 for ChNW and rChNW2, pH 7 for CNC and rCNC2). However, the content of CNC in rChNW2 was lower than the content of ChNW in rCNC2, so the XRD pattern for rChNW2 differed from that of the original ChNW significantly while the XRD pattern for rCNC2 was close to that of the original CNC.

Properties of Films. PET films coated with original or recycled materials all had better oxygen barrier properties than uncoated PET. The OP values for all films are shown in Figure 5. The film thicknesses and statistical analysis results on mean oxygen permeability are shown in Tables S4 and S5, respectively. ChNWs and CNCs applied as individual single layers, a bilayer, or a single layer of the blend formed oxygen barrier coatings consisting of densely packed lamellae of nanoparticles on PET substrates, as shown in cross-sectional SEM images in Figure S4. No significant difference was observed in the microstructure for all of the coatings. For films coated with original materials, the average OP value of a bilayer-coated PET film (i.e., 5.2 ± 0.4 $cm^3 \cdot \mu m/m^2/day/kPa$) was lower than the OP values of single-layer-coated films (i.e., 12.6 ± 0.9 and 5.9 ± 0.7 $cm^3 \cdot \mu m/m^2/day/kPa$ for PET-ChNW and PET-CNC, respectively), though no statistically significant difference was shown between OP values of PET-CNC and PET-ChNW-CNC. This trend corresponds with previous studies on combining nanochitin and nanocellulose as alternating layers.[15,20,22] It is hypothesized to be the result of a denser structure at the interface of oppositely charged nanochitin and nanocellulose, which was verified by thinner bilayer thicknesses (i.e., ~6 μm) compared to the sum of single-layer-coating thicknesses, i.e., ~8 μm (~5 μm for ChNW and ~3 μm for CNC), as shown in Table S4. The OP value of PET-blend (i.e., 10.2 ± 1.2 $cm^3 \cdot \mu m/m^2/day/kPa$) is lower than that of PET-ChNW and higher than that of PET-CNC. This also corresponds to the trend in previous studies that the blends of short ChNF and CNC with different mass ratios had OP values between those of individual materials.[9] Thus, applying ChNW and CNC as bilayers rather than blend provides a better oxygen barrier performance.

For films coated with recycled materials, the same trend in OP was observed though the average values changed. PET films coated with rChNW1 and rblend had similar OP values as films coated with original materials. PET films coated with rCNC1 had an OP value (6.9 ± 0.2 $cm^3 \cdot \mu m/m^2/day/kPa$) that was 17% higher than that of PET-CNC. Since CNC is very stable to desulfation under neutral conditions,[35] which is also supported by elemental analysis results (Table S3), the increase of OP of PET-rCNC1 is less likely to be caused by CNC degradation in suspension. A possible reason is that the rCNC1 had lower electrostatic repulsion than the original CNC, which might be due to ions released from the gel layer, as indicated by the ζ potential values (Figure 3a), and thus the nanocrystals packed more randomly in the coating. The PET-rChNW2-rCNC2 had an average OP (6.6 ± 0.7 $cm^3 \cdot \mu m/m^2/day/kPa$) that was 27% higher than that of PET-ChNW-CNC. Two reasons explain this higher OP: (1) recycling caused a decrease in the oxygen barrier property of CNC as shown by rCNC1 and (2) suspensions of rChNW2 and rCNC2 were both mixtures of ChNWs and CNCs, and OP data for original coated films show that the blend had higher OP than a bilayer consisting of unmixed ChNWs and CNCs. However, although recycling resulted in a loss of oxygen barrier property, the PET-rCNC1 and PET-rChNW2-rCNC2 films had OP values that were 60 and 62% lower than that of uncoated PET, respectively, suggesting that recycled materials still performed as an efficient oxygen barrier on PET substrates. Furthermore, in most cases of recycling, the recycled materials are blended with virgin materials rather than at a 100% loading, so the loss of oxygen barrier property for rCNC1 and rChNW2-rCNC2 might be compensated in this way.

The water vapor barrier properties of the coated films, however, were not significantly different from those of the uncoated PET, as shown in Figure 5b. The statistical analysis results on the mean water vapor transmission rate (WVTR) are shown in Table S6. For PET films coated with different

https://doi.org/10.1021/acssuschemeng.3c02457
ACS Sustainable Chem. Eng. 2023, 11, 10874−10883

materials in different formulations, the changes in WVTR values are within the error bars, though PET films coated with recycled materials had WVTR values that were on average 7% lower than those of PET films coated with original materials. This is because the PET substrate is a good moisture barrier and comprised 75−90% of the total film thickness, while chitin and cellulose are hydrophilic and comprised a smaller portion of film thickness. Thus, the PET substrate dominated the water vapor barrier property of the coated films.

In most studies on the recycling of coated films where cellulose, chitin, or chitosan is involved, experiments mainly focused on the separation of the coating from the substrate, and changes in properties of the polysaccharides were not studied.[22,49] Only one previous work involves the recycling of CNF coatings.[51] However, in the cited paper, the CNF coating became completely blended with the substrate material (polyethylene, PE) during recycling steps that involved film shredding, mixing with virgin PE, and extrusion; the recycled blend films had oxygen transmission rates that were 2.4−32 times larger than the original coated films.[51] Our work, thus, proposes for the first time a method for recycling the coating materials where the recycled materials are separated from the substrate and have OP values less than 27% higher than the original materials.

In this work, the PET films coated with a bilayer, either of original or of recycled materials, have OP values that are superior or comparable to the results in some previous studies utilizing chitin- and cellulose-based materials as alternating coatings. For instance, the polypropylene (PP) film coated with 20 bilayers of ChNW and TEMPO-oxidized CNF had an OP of 7.76 $cm^3 \cdot \mu m/m^2/day/kPa$ at 23 °C and 50% RH and a WVTR of 128 $g \cdot \mu m/m^2/day$ at 30 °C and 50% RH.[17] However, different substrates, coating structures (i.e., number of bilayers), and testing conditions make it difficult to directly compare the gas barrier properties of the coatings in different studies, which has been discussed in detail in our previous studies.[19,21] Additionally, the PET film coated with recycled materials as a bilayer had oxygen and water vapor barrier properties that are suitable for the packaging of many types of food. The normalized oxygen transmission rate (OTR) and WVTR for a 100-μm-thick film under room atmosphere are 1.4 $cm^3/m^2/day$ and 1.36 $g/m^2/day$, respectively, assuming 23 °C, 50% RH, and 21 kPa for the driving force of O_2. This film has gas barrier properties that satisfy the requirements for fresh produce, meat, bakery products, cheese, peanuts, and part of instant coffee.[23] Its gas barrier properties are superior or comparable to most other commercial plastics for food packaging, such as PE, PP, polystyrene (PS), and PVC, but there is still large room for improvement comparing to EVOH as shown in Table S7.[52]

The optical properties of the coated films generally corresponded well with the optical properties of the coating suspensions. The transmittance and haze spectra for coated films and the values of average transmittance and haze in the range of 400−700 nm are shown in Figure S5 and Table S8, respectively. Most obviously, the PET-rChNW2-rCNC2 film had the lowest average transmittance (84.6%) and highest average haze (36.4%), correlating with the increased opacity of the rCNC2 suspension due to larger particle size. The other coated films all had high transmittances (>80%), and recycling did not significantly change the transmittances. Though recycling resulted in a slight increase in the haze, these coated films had low haze (<10%) in the range of 400−700 nm, except PET-rChNW2-rCNC2 (36.4%). Generally, the high transmittance and low haze of the coated films also make them potential substitutes for applications other than food packaging, such as electrochromic device packaging.[53]

Admittedly, numerous challenges need to be overcome to use PET-ChNW-CNC in practice. For instance, handling a waste stream usually involves a prewashing step to remove package contents, i.e., food waste, using water or an alkaline solution.[26,27] This will result in the contamination and some loss of the CNC material. However, because ChNWs have a low dispersibility in water and alkaline solution, they will be only slightly removed during these prewashing steps. Additionally, a current practice to protect the oxygen barrier is to layer another material as a package seal and the liquid barrier. The use of an internal seal would also help prevent dispersion of CNCs back into the packaged products. The selection of an ideal seal, the technique of tying the seal layer with the coating, and its removal and recovery are also challenges to be addressed before realizing the manufacturing and recycling of our product. The main advance of this work is demonstrating that the ChNW-CNC barrier coatings can be removed, recovered, and recoated. This concept is an essential step to realizing the application of ChNW and CNC in practice.

Influence of Multiple Recycling Runs on Suspension and Film Properties. Because the changes in film gas barrier properties were observed after the recycling process, it is interesting to know the influence of additional recycling runs on the properties. Here, the PET coated with a single layer of CNC was selected as the model because of its simple film structure and good oxygen barrier property.

The comparison of properties of the original or recycled CNCs is shown in Figure S6 and Table S9. The original and recycled CNCs had similar XRD patterns and high CrIs (65−70%), suggesting recycling for multiple runs did not change the crystalline structure of CNCs significantly. However, with an increasing number of recycling runs, the R_h increased from 50 ± 2 to 129 ± 11 nm, suggesting more aggregation and leading to a decreased suspension transmittance. The aggregation is likely due to the formation of hydrogen bonds during drying. The zeta potential increased from −27.5 ± 2.4 to −24.9 ± 0.4 mV, which suggests not only the weaker repulsion between CNCs due to the screening effect of released ions from the gel layer but also CNC aggregation which reduces exposed charged groups. Regarding the rheological properties, the original CNC and rCNC1 behaved as Newtonian fluids at shear rates greater than 1 s^{-1}, but 2rCNC1 and 3rCNC1 had shear-thinning behavior at shear rates ranging from 0.1 to 300 s^{-1} and from 0.1 to 30 s^{-1}, respectively (Figure S6c). This is probably because the aggregates of CNCs in 2rCNC1 and 3rCNC1 had larger aspect ratios; they may align under the shear force and may break into smaller aggregates or individual CNCs at high shear rates.[54] The hypothesis of broken CNC aggregates under shear is supported by the average R_h values for 2rCNC1 and 3rCNC1 after passing through the nozzle during spraying (Table S9), which were smaller than R_h values of unsprayed suspensions.

Regarding gas barrier properties shown in Figure 6, the OP values of the films coated with recycled materials were on average 36% higher than that of the original PET-CNC, while the water vapor barrier property did not change significantly. The higher OP is likely attributed to the less ordered structure in the recycled coatings due to the weaker electrostatic repulsion between CNCs as discussed earlier. Based on our

https://doi.org/10.1021/acssuschemeng.3c02457
ACS Sustainable Chem. Eng. 2023, 11, 10874−10883

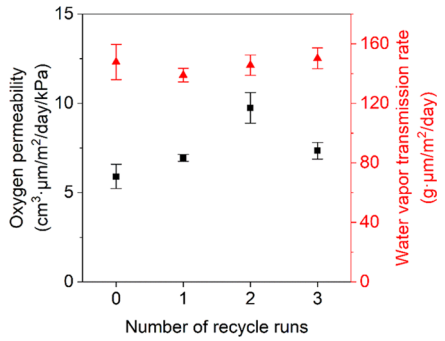

Figure 6. Oxygen permeabilities (black squares) and water vapor transmission rates (red triangles) for PET films coated with CNC recycled for up to three rounds.

previous study on ChNW coatings,[19] where ChNWs with shorter lengths resulted in lower OP of the coated films, it was expected that CNCs with larger dimensions had poorer gas barrier properties. However, although the properties of the suspensions changed with recycling runs, there is no statistically significant difference in OP among the recycled coated film samples (Table S10). Two reasons may explain this: (1) though the average R_h became higher after more recycling runs, there remained individual CNCs which filled in the voids between larger aggregates and still formed a dense coating and (2) the CNC aggregates may break into smaller aggregates or individual CNCs when the suspension passed through the nozzle during spray coating. Among the coated films with recycled materials, PET-2rCNC1 had the highest average OP value (i.e., 9.7 ± 0.9 $cm^3 \cdot \mu m/m^2/day/kPa$). A possible explanation is that there were more aggregates in 2rCNC1 than in other recycled suspensions as indicated by its highest viscosity, resulting in a less dense coating. Nevertheless, after three recycling runs, PET-3rCNC1 had an OP (i.e., 7.5 ± 0.5 $cm^3 \cdot \mu m/m^2/day/kPa$) which was only 24% higher than that of PET-rCNC1 and 58% lower than that of uncoated PET. Thus, the CNC coating still functioned as an effective oxygen barrier on PET after being recycled for three runs.

Sustainability Metrics. Recycling the ChNW and CNC coatings will result in a significant decrease in energy consumption compared to producing the materials. The energy consumed for recycling ChNW and CNC is estimated to be 258 and 204 MJ per kilogram of dry ChNW and CNC, respectively. While a technoeconomic analysis for producing ChNW by alkaline-assisted deacetylation is unavailable, the energy consumption for producing ChNW is estimated based on a previous report on producing chitosan.[55] The total energy consumed for producing ChNW suspension containing 1 kg of solid is estimated to be 1746 MJ. Details of the calculation of the energy consumption are available in the Supporting Information. For producing CNC with the FPL pilot plant scale-up production line, the total energy consumed is 992.7 MJ per kilogram of CNC.[56] Thus, recycling ChNW and CNC from the coating using the aqueous-based method in this work could save 85 and 79% of energy compared to producing ChNW and CNC, respectively.

CONCLUSIONS

In this work, the recycling of layered CNC and ChNW coatings was explored by selective solvent dissolution for the first time. Different formulations of ChNW and CNC coatings, including single layers of individual materials, a bilayer of ChNW and CNC, and a single layer of the blend of ChNW and CNC, were effectively separated from the PET substrates by a simple stirring-filtration process. Water and HOAc aqueous solution were used to remove the single layer of CNC and ChNW-containing layers, respectively. The recovered coating materials were recycled by concentrating and redispersing via sonication, followed by recoating on PET. The recycled coated films still improved oxygen barrier properties relative to neat PET, though the oxygen barrier properties decreased after recycling. The PET coated with recycled bilayer had gas barrier properties that meet the requirement for packaging of many types of food, such as fresh produce, meat, and instant coffee.

This study utilizes a simple method for not only recycling the relatively more costly CNC and ChNW barrier coatings but also could support development of a process for recycling the PET substrates by promoting the separation of the multilayer structure beforehand. Future challenges that remain to be addressed stem from the likely need in a packaging application to cover the CNC and ChNW layers with an inner seal layer that would provide for package closure and protection from liquid water, as well as the potential utilization of adhesives between layers. In addition, the cross-contamination of ChNW and CNC into one another suspension when recycled from a bilayer coating is still a problem to be solved, since it leads to particle aggregation in suspensions and finally a loss of oxygen barrier property of the recycled bilayer-coated film. One possible method is to apply an alkaline solution for separating the CNC layer, in which ChNW has poorer solubility and precipitates due to deprotonation. Thus, the selection of appropriate solvents for recycling multilayer coatings, which requires a high selectivity and low reactivity with recycled material, and the feasibility of recoating the resulting suspension, is an interesting topic for future exploration.

ASSOCIATED CONTENT

Supporting Information

The Supporting Information is available free of charge at https://pubs.acs.org/doi/10.1021/acssuschemeng.3c02457.

Additional supporting results including properties of ChNW and CNC, XRD characterization method, photographs of suspensions, elemental analysis results, FT-IR spectra, viscosities of suspensions, SEM images, film thicknesses, statistical significance analyses for film gas barrier properties, and calculations of the energy consumption (PDF)

AUTHOR INFORMATION

Corresponding Author

J. Carson Meredith − *School of Chemical and Biomolecular Engineering, Georgia Institute of Technology, Atlanta, Georgia 30332, United States; Renewable Bioproducts Institute, Georgia Institute of Technology, Atlanta, Georgia 30332, United States;* orcid.org/0000-0003-2519-5003; Email: carson.meredith@chbe.gatech.edu

Authors

Yue Ji − *School of Chemical and Biomolecular Engineering, Georgia Institute of Technology, Atlanta, Georgia 30332, United States;* orcid.org/0000-0003-4775-497X

D. Eric Shen − *School of Chemistry and Biochemistry, Georgia Institute of Technology, Atlanta, Georgia 30332, United States;* orcid.org/0000-0002-8318-898X

Yang Lu − *School of Chemical and Biomolecular Engineering, Georgia Institute of Technology, Atlanta, Georgia 30332, United States*

Gregory T. Schueneman − *Forest Products Laboratory, U.S. Forest Service, Madison, Wisconsin 53726, United States;* orcid.org/0000-0002-6390-5240

Meisha L. Shofner − *School of Materials Science and Engineering, Georgia Institute of Technology, Atlanta, Georgia 30332, United States; Renewable Bioproducts Institute, Georgia Institute of Technology, Atlanta, Georgia 30332, United States;* orcid.org/0000-0003-2774-4379

Complete contact information is available at: https://pubs.acs.org/10.1021/acssuschemeng.3c02457

Notes

The authors declare no competing financial interest.

■ ACKNOWLEDGMENTS

The authors acknowledge the Department of Energy (DOE) for the financial support of this work (EE0008494). This work was performed in part at the Georgia Tech Institute for Electronics and Nanotechnology, a member of the National Nanotechnology Coordinated Infrastructure (NNCI), which is supported by the National Science Foundation (ECCS-2025462). This work was performed in part at the Organic Materials Characterization Laboratory and the Biomechanics Core at Georgia Tech.

■ REFERENCES

(1) Robertson, G. L. 4 - Optical, Mechanical and Barrier Properties of Thermoplastic Polymers. In *Food Packaging: Principles and Practice*, 3rd ed.; Taylor & Francis Group: Bosa Roca, United States, 2012; pp 91−130 DOI: 10.1201/b21347.

(2) Kirwan, M. J.; Plant, S.; Strawbridge, J. W. Plastics in Food Packaging. In *Food and Beverage Packaging Technology*; Coles, R.; Kirwan, M., Eds.; Wiley-Blackwell: Oxford, 2011; pp 157−212 DOI: 10.1002/9781444392180.ch7.

(3) Chamas, A.; Moon, H.; Zheng, J. J.; Qiu, Y.; Tabassum, T.; Jang, J. H.; Abu-Omar, M.; Scott, S. L.; Suh, S. Degradation Rates of Plastics in the Environment. *ACS Sustainable Chem. Eng.* **2020**, *8*, 3494−3511.

(4) Siracusa, V.; Blanco, I. Bio-Polyethylene (Bio-PE), Bio-Polypropylene (Bio-PP) and Bio-Poly(ethylene terephthalate) (Bio-PET): Recent Developments in Bio-Based Polymers Analogous to Petroleum-Derived Ones for Packaging and Engineering Applications. *Polymers* **2020**, *12*, 1641.

(5) Leal Filho, W.; Saari, U.; Fedoruk, M.; Iital, A.; Moora, H.; Kloga, M.; Voronova, V. An overview of the problems posed by plastic products and the role of extended producer responsibility in Europe. *J. Cleaner Prod.* **2019**, *214*, 550−558.

(6) Moon, R. J.; Martini, A.; Nairn, J.; Simonsen, J.; Youngblood, J. Cellulose nanomaterials review: Structure, properties and nanocomposites. *Chem. Soc. Rev.* **2011**, *40*, 3941−3994.

(7) Ifuku, S.; Saimoto, H. Chitin nanofibers: preparations, modifications, and applications. *Nanoscale* **2012**, *4*, 3308−3318.

(8) Yang, W. S.; Gao, Y.; Zuo, C.; Deng, Y. L.; Dai, H. Q. Thermally-induced cellulose nanofibril films with near-complete ultraviolet-blocking and improved water resistance. *Carbohydr. Polym.* **2019**, *223*, No. 115050.

(9) Satam, C. C.; Irvin, C. W.; Coffey, C. J.; Geran, R. K.; Ibarra-Rivera, R.; Shofner, M. L.; Meredith, J. C. Controlling Barrier and Mechanical Properties of Cellulose Nanocrystals by Blending with Chitin Nanofibers. *Biomacromolecules* **2020**, *21*, 545−555.

(10) Chowdhury, R. A.; Nuruddin, M.; Clarkson, C.; Montes, F.; Howarter, J.; Youngblood, J. P. Cellulose Nanocrystal (CNC) Coatings with Controlled Anisotropy as High-Performance Gas Barrier Films. *ACS Appl. Mater. Interfaces* **2019**, *11*, 1376−1383.

(11) Duan, B.; Chang, C. Y.; Ding, B. B.; Cai, J.; Xu, M.; Feng, S. C.; Ren, J. Z.; Shi, X. W.; Du, Y. M.; Zhang, L. N. High strength films with gas-barrier fabricated from chitin solution dissolved at low temperature. *J. Mater. Chem. A* **2013**, *1*, 1867−1874.

(12) Tran, T. H.; Nguyen, H.-L.; Hwang, D. S.; Lee, J. Y.; Cha, H. G.; Koo, J. M.; Hwang, S. Y.; Park, J.; Oh, D. X. Five different chitin nanomaterials from identical source with different advantageous functions and performances. *Carbohydr. Polym.* **2019**, *205*, 392−400.

(13) Wu, J.; Zhang, K.; Girouard, N.; Meredith, J. C. Facile Route to Produce Chitin Nanofibers as Precursors for Flexible and Transparent Gas Barrier Materials. *Biomacromolecules* **2014**, *15*, 4614−4620.

(14) Yu, Z. Y.; Ji, Y.; Bourg, V.; Bilgen, M.; Meredith, J. C. Chitin- and cellulose-based sustainable barrier materials: a review. *Emergent Mater.* **2020**, *3*, 919−936.

(15) Kim, T.; Tran, T. H.; Hwang, S. Y.; Park, J.; Oh, D. X.; Kim, B. S. Crab-on-a-Tree: All Biorenewable, Optical and Radio Frequency Transparent Barrier Nanocoating for Food Packaging. *ACS Nano* **2019**, *13*, 3796−3805.

(16) Li, F.; Biagioni, P.; Finazzi, M.; Tavazzi, S.; Piergiovanni, L. Tunable green oxygen barrier through layer-by-layer self-assembly of chitosan and cellulose nanocrystals. *Carbohydr. Polym.* **2013**, *92*, 2128−2134.

(17) Nguyen, H. L.; Tran, T. H.; Hao, L. T.; Jeon, H.; Koo, J. M.; Shin, G.; Hwang, D. S.; Hwang, S. Y.; Park, J.; Oh, D. X. Biorenewable, transparent, and oxygen/moisture barrier nanocellulose/nanochitin-based coating on polypropylene for food packaging applications. *Carbohydr. Polym.* **2021**, *271*, No. 118421.

(18) Thuy, V. T. T.; Hao, L. T.; Jeon, H.; Koo, J. M.; Park, J.; Lee, E. S.; Hwang, S. Y.; Choi, S.; Park, J.; Oh, D. X. Sustainable, self-cleaning, transparent, and moisture/oxygen-barrier coating films for food packaging. *Green Chem.* **2021**, *23*, 2658−2667.

(19) Ji, Y.; Waters, S.; Lim, E.; Lang, A. W.; Ciesielski, P. N.; Shofner, M. L.; Reynolds, J. R.; Meredith, J. C. Minimizing Oxygen Permeability in Chitin/Cellulose Nanomaterial Coatings by Tuning Chitin Deacetylation. *ACS Sustainable Chem. Eng.* **2022**, *10*, 124−133.

(20) Satam, C. C.; Irvin, C. W.; Lang, A. W.; Jallorina, J. C. R.; Shofner, M. L.; Reynolds, J. R.; Meredith, J. C. Spray-Coated Multilayer Cellulose Nanocrystal-Chitin Nanofiber Films for Barrier Applications. *ACS Sustainable Chem. Eng.* **2018**, *6*, 10637−10644.

(21) Ji, Y.; Shen, D. E.; Young, E. K.; Goins, C. L.; Reynolds, J. R.; Shofner, M. L.; Meredith, J. C. Optimization of spray-coated nanochitin/nanocellulose films as renewable oxygen barrier layers via thermal treatment. *Mater. Adv.* **2022**, *3*, 8351−8360.

(22) Yu, Z.; Ji, Y.; Meredith, J. C. Multilayer Chitin−Chitosan−Cellulose Barrier Coatings on Poly(ethylene terephthalate). *ACS Appl. Polym. Mater.* **2022**, *4*, 7182−7190.

(23) Wang, J.; Gardner, D. J.; Stark, N. M.; Bousfield, D. W.; Tajvidi, M.; Cai, Z. Moisture and Oxygen Barrier Properties of Cellulose Nanomaterial-Based Films. *ACS Sustainable Chem. Eng.* **2018**, *6*, 49−70.

(24) Vollmer, I.; Jenks, M. J. F.; Roelands, M. C. P.; White, R. J.; van Harmelen, T.; de Wild, P.; van der Laan, G. P.; Meirer, F.; Keurentjes, J. T. F.; Weckhuysen, B. M. Beyond Mechanical Recycling: Giving New Life to Plastic Waste. *Angew. Chem., Int. Ed.* **2020**, *59*, 15402−15423.

(25) Walker, T. W.; Frelka, N.; Shen, Z. Z.; Chew, A. K.; Banick, J.; Grey, S.; Kim, M. S.; Dumesic, J. A.; Van Lehn, R. C.; Huber, G. W. Recycling of multilayer plastic packaging materials by solvent-targeted recovery and precipitation. *Sci. Adv.* **2020**, *6*, No. aba7599.

(26) Bacchiocchi, L.; Pozzi, G. *Additive for Use in Wash Step of PET Recycling Process*, US Patent US20130261197A1, October 3, 2013.

(27) Welle, F. Twenty years of PET bottle to bottle recycling-An overview. *Resour., Conserv. Recycl.* **2011**, *55*, 865−875.

(28) Statista. Price of polyethylene terephthalate (PET) worldwide from 2017 to 2020 with estimatedfigures for 2021 to 2022. 2021. https://www.statista.com/statistics/1171088/price-polyethylene-terephthalate-forecast-globally/ (accessed October 18, 2022).
(29) Nelson, K.; Retsina, T.; Iakovlev, M.; van Heiningen, A.; Deng, Y.; Shatkin, J. A.; Mulyadi, A. American Process: Production of Low Cost Nanocellulose for Renewable, Advanced Materials Applications. In *Materials Research for Manufacturing: An Industrial Perspective of Turning Materials into New Products*; Madsen, L. D.; Svedberg, E. B., Eds.; Springer International Publishing: Cham, 2016; pp 267−302 DOI: 10.1007/978-3-319-23419-9_9.
(30) Zuorro, A.; Moreno-Sader, K. A.; Gonzalez-Delgado, A. D. Economic Evaluation and Techno-Economic Sensitivity Analysis of a Mass Integrated Shrimp Biorefinery in North Colombia. *Polymers* **2020**, *12*, No. 2397.
(31) Segal, L.; Creely, J. J.; Martin, A. E.; Conrad, C. M. An Empirical Method for Estimating the Degree of Crystallinity of Native Cellulose Using the X-Ray Diffractometer. *Text. Res. J.* **1959**, *29*, 786−794.
(32) Zhang, Y. Q.; Xue, C. H.; Xue, Y.; Gao, R. C.; Zhang, X. L. Determination of the degree of deacetylation of chitin and chitosan by X-ray powder diffraction. *Carbohydr. Res.* **2005**, *340*, 1914−1917.
(33) Beck, S.; Bouchard, J.; Berry, R. Dispersibility in Water of Dried Nanocrystalline Cellulose. *Biomacromolecules* **2012**, *13*, 1486−1494.
(34) Bhattacharjee, S. DLS and zeta potential - What they are and what they are not? *J. Controlled Release* **2016**, *235*, 337−351.
(35) Beck, S.; Bouchard, J. Auto-catalyzed acidic desulfation of cellulose nanocrystals. *Nord. Pulp Pap. Res. J.* **2014**, *29*, 6−14.
(36) Beck, S.; Bouchard, J.; Berry, R. Controlling the Reflection Wavelength of Iridescent Solid Films of Nanocrystalline Cellulose. *Biomacromolecules* **2011**, *12*, 167−172.
(37) Labet, M.; Thielemans, W. Improving the reproducibility of chemical reactions on the surface of cellulose nanocrystals: ROP of epsilon-caprolactone as a case study. *Cellulose* **2011**, *18*, 607−617.
(38) Mujtaba Karim, S.; Samuel, R. Absorption spectra of the sulphite and sulphate ions. *Proc. Indian Acad. Sci., Sect. A* **1934**, *1*, 398−406.
(39) Nielsen, E. B.; Schellman, J. A. Absorption Spectra of Simple Amides and Peptides. *J. Phys. Chem. A* **1967**, *71*, 2297−2304.
(40) Peng, Y. C.; Via, B. The Effect of Cellulose Nanocrystal Suspension Treatment on Suspension Viscosity and Casted Film Property. *Polymers* **2021**, *13*, No. 2168.
(41) King, T. A. 7 - Photon Correlation Spectroscopy: Technique and Scope. In *Comprehensive Polymer Science and Supplements*; Allen, G.; Bevington, J. C., Eds.; Pergamon: Amsterdam, 1989; pp 911−935 DOI: 10.1016/B978-0-08-096701-1.00007-0.
(42) Klemm, D.; Kramer, F.; Moritz, S.; Lindstrom, T.; Ankerfors, M.; Gray, D.; Dorris, A. Nanocelluloses: A New Family of Nature-Based Materials. *Angew. Chem., Int. Ed.* **2011**, *50*, 5438−5466.
(43) Kasaai, M. R. Various Methods for Determination of the Degree of N-Acetylation of Chitin and Chitosan: A Review. *J. Agric. Food Chem.* **2009**, *57*, 1667−1676.
(44) Tsaih, M. L.; Chen, R. H. Effects of ionic strength and pH on the diffusion coefficients and conformation of chitosans molecule in solution. *J. Appl. Polym. Sci.* **1999**, *73*, 2041−2050.
(45) Zhong, T. H.; Wolcott, M. P.; Liu, H.; Wang, J. W. Developing chitin nanocrystals for flexible packaging coatings. *Carbohydr. Polym.* **2019**, *226*, No. 115276.
(46) Park, S.; Baker, J. O.; Himmel, M. E.; Parilla, P. A.; Johnson, D. K. Cellulose crystallinity index: measurement techniques and their impact on interpreting cellulase performance. *Biotechnol. Biofuels* **2010**, *3*, No. 10.
(47) Butchosa, N.; Brown, C.; Larsson, P. T.; Berglund, L. A.; Bulone, V.; Zhou, Q. Nanocomposites of bacterial cellulose nanofibers and chitin nanocrystals: fabrication, characterization and bactericidal activity. *Green Chem.* **2013**, *15*, 3404−3413.
(48) Gupta, N. S. *Chitin: Formation and Diagenesis*; Springer Science & Business Media, 2010; Vol. *34*.
(49) Irvin, C. W.; Satam, C. C.; Liao, J. S.; Russo, P. S.; Breedveld, V.; Meredith, J. C.; Shofner, M. L. Synergistic Reinforcement of Composite Hydrogels with Nanofiber Mixtures of Cellulose Nanocrystals and Chitin Nanofibers. *Biomacromolecules* **2021**, *22*, 340−352.
(50) Gicquel, E.; Bras, J.; Rey, C.; Putaux, J. L.; Pignon, F.; Jean, B.; Martin, C. Impact of sonication on the rheological and colloidal properties of highly concentrated cellulose nanocrystal suspensions. *Cellulose* **2019**, *26*, 7619−7634.
(51) Vartiainen, J.; Pasanen, S.; Kentta, E.; Vaha-Nissi, M. Mechanical recycling of nanocellulose containing multilayer packaging films. *J. Appl. Polym. Sci.* **2018**, *135*, No. 46237.
(52) Lange, J.; Wyser, Y. Recent innovations in barrier technologies for plastic packaging - a review. *Packag. Technol. Sci.* **2003**, *16*, 149−158.
(53) Lang, A. W.; Ji, Y.; Dillon, A. C.; Satam, C. C.; Meredith, J. C.; Reynolds, J. R. Photostability of Ambient-Processed, Conjugated Polymer Electrochromic Devices Encapsulated by Bioderived Barrier Films. *ACS Sustainable Chem. Eng.* **2021**, *9*, 2937−2945.
(54) Iwamoto, S.; Lee, S. H.; Endo, T. Relationship between aspect ratio and suspension viscosity of wood cellulose nanofibers. *Polym. J.* **2014**, *46*, 73−76.
(55) Gomez-Rios, D.; Barrera-Zapata, R.; Rios-Estepa, R. Comparison of process technologies for chitosan production from shrimp shell waste: A techno-economic approach using Aspen Plus (R). *Food Bioprod. Process.* **2017**, *103*, 49−57.
(56) Gu, H.; Reiner, R.; Bergman, R.; Rudie, A. In *LCA Study for pilot scale production of cellulose nano crystals (CNC) from wood pulp, Proceedings from the LCA XV Conference - A bright green future, Vancouver, British Columbia, Canada*, 2015; pp 33−42.